Acta Crystallographica Section F
Structural Biology and Crystallization Communications
ISSN 1744-3091

Complexes of the copper-containing amine oxidase from *Arthrobacter globiformis* with the inhibitors benzylhydrazine and tranylcypromine

David B. Langley,[a] Daniel M. Trambaiolo,[a] Anthony P. Duff,[a] David M. Dooley,[b] Hans C. Freeman[a] and J. Mitchell Guss[a]*

[a]School of Molecular and Microbial Biosciences, University of Sydney, Australia, and [b]Department of Chemistry and Biochemistry, Montana State University, USA

Correspondence e-mail: m.guss@usyd.edu.au

Received 3 April 2008
Accepted 23 May 2008

PDB References: *A. globiformis* amine oxidase, benzylhydrazine complex, 1w5z, r1w5zsf; tranylcypromine complex, 1w4n, r1w4nsf.

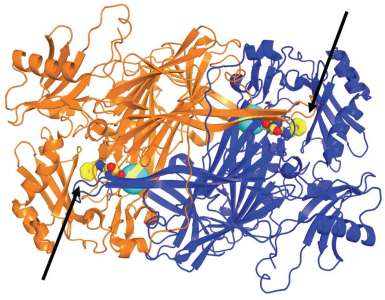

Complexes of *Arthrobacter globiformis* amine oxidase (AGAO) with the inhibitors benzylhydrazine and tranylcypromine (an antidepressant drug) have been refined at 1.86 and 1.65 Å resolution, respectively. Both inhibitors form covalent adducts with the TPQ cofactor. A tyrosine residue, proposed to act as a gate to the AGAO active site, is in its open conformation.

1. Introduction

Amine oxidases (AOs) catalyse the oxidative deamination of amines to the corresponding aldehydes, with the subsequent reduction of O_2 to H_2O_2 and the release of NH_4^+,

$$R\mathrm{CH_2NH_3^+} + \mathrm{O_2} + \mathrm{H_2O} \rightarrow R\mathrm{CHO} + \mathrm{NH_4^+} + \mathrm{H_2O_2}. \qquad (1)$$

AOs are found in all kingdoms of life and can be broadly categorized into two groups: the quinone-containing copper amine oxidases (CuAOs) and the flavin-dependent monoamine oxidases (MAOs). The CuAOs can be further categorized according to the nature of the quinone cofactor, which is either 2,4,5-trihydroxyphenylalanine-quinone (TPQ) or lysyltyrosylquinone (LTQ), both of which are spontaneously formed by post-translational modifications of active-site amino-acid residues (Dove *et al.*, 1996; Cai & Klinman, 1994). In eukaryotes the TPQ-containing enzymes contribute to a variety of functions including cell adhesion and detoxification, while in bacteria they are thought to be involved primarily in the liberation of dietary nitrogen. The vertebrate LTQ-containing 'lysyl oxidase' enzymes are involved in the maturation of connective tissue by the oxidation of lysine residues in collagen. In mammals, MAOs are found in the outer mitochondrial membrane and are particularly important in the oxidation of arylalkylamine neurotransmitters such as nor-epinephrine, dopamine and serotonin. As a result, MAOs are targets for antidepressant drugs which slow the degradation of such 'pleasure' molecules. Tranylcypromine (TCP) has been used clinically for the treatment of depression. It inhibits not only its target MAO but also TPQ-containing CuAOs. This may account for its side effects, which have led to its replacement by newer drugs (Knowles *et al.*, 2007). However, these newer drugs are often less effective and TCP is still used under careful supervision to treat severe depression.

Three-dimensional structures of TPQ-containing CuAOs have been determined from bacteria [*Escherichia coli* (ECAO; Parsons *et al.*, 1995) and *Arthrobacter globiformis* (AGAO; Wilce *et al.*, 1997)], yeasts [*Pichia augusta* (formerly *Hansenula polymorpha*; HPAO; Li *et al.*, 1998) and *P. pastoris* (PPLO; Duff *et al.*, 2003)], a plant (*Pisum sativum*; PSAO; Kumar *et al.*, 1996) and mammals [cow (BSAO; Lunelli *et al.*, 2005) and human (VAP1, also known as SSAO or 'semicarbazide-sensitive amine oxidase'; Jakobsson *et al.*, 2005; Airenne *et al.*, 2005)]. No structure of an LTQ-CuAO has yet been determined. Known MAO structures include those of human MAO-A and MAO-B, the latter as a complex with TCP (Binda *et al.*, 2003, 2005).

CuAOs utilize a ping-pong mechanism that can be split into reductive and oxidative half-reactions (Dove & Klinman, 2001). In the well understood reductive half-reaction, the amine substrate forms a Schiff base with TPQ and a proton is subsequently abstracted from the methylene C atom bonded to the primary amine group by a

conserved aspartic acid residue acting as a base (Asp298 in AGAO). Irreversible hydrazine-derivative inhibitors of CuAOs trap the enzyme in a covalent adduct analogous to the substrate Schiff-base complex. In the structure of the 2-hydrazinopyridine (2-HP) complex of ECAO, the TPQ cofactor is linked covalently to 2-HP *via* the 5-position of the quinone ring (Wilmot *et al.*, 1997). A similar link is observed in the complex of TCP and ECAO (Wilmot *et al.*, 2004). In this case, the TCP acts as a reversible inhibitor or nonhydrolysable substrate analogue.

The amine oxidase from *A. globiformis* was initially described as 'phenylethylamine' amine oxidase owing to its substrate preference for small primary amines attached to aromatic rings. The structure of AGAO has been determined in crystals of the apoenzyme and holoenzyme (Wilce *et al.*, 1997), Ni- and Co-substituted enzymes (Okajima *et al.*, 2005), stages in the biogenesis of the TPQ cofactor (Kim *et al.*, 2002), mutants lacking key Cu-ligand residues (Matsunami *et al.*, 2004), a xenon derivative (Duff *et al.*, 2004), an inactive mutant with bound tyramine (Murakawa *et al.*, 2006) and complexes with both covalently and noncovalently bound inhibitors (Contakes *et al.*, 2005; O'Connell *et al.*, 2004). In all the structures AGAO is a dimer, in which each subunit is composed of three domains: D2, D3 and D4. A D1 domain has so far been found only in ECAO. Loops from the D4 domain in one subunit extend across the D4 domain in the other subunit to form a tightly integrated central domain that contains two active sites, each defined by the presence of a TPQ cofactor and an active-site Cu atom. A channel for the entry of substrate leads from the protein surface to the TPQ. A 'lake' of water molecules is enclosed at the dimer interface and has been suggested as a possible route for the entrance of O_2 to and the exit of H_2O_2 from the active site (Wilce *et al.*, 1997).

In this paper, we present the crystal structures of complexes of AGAO with benzylhydrazine (BH) and tranylcypromine (TCP) (Fig. 1). After the structure of the AGAO complex of BH had been deposited in the Protein Data Bank, another group deposited an isomorphous structure of this complex (PDB code 2e2v) without an accompanying publication.

2. Materials and methods

2.1. Enzyme purification and crystallization

AGAO was overexpressed recombinantly as a C-terminal Strep-tagII fusion protein. It was purified and concentrated using published protocols to a concentration of ∼10 mg ml^{-1} in 50 m*M* 4-(2-hydroxyethyl)-1-piperazineethanesulfonic acid (HEPES) buffer pH 7.0 (Juda *et al.*, 2001). The purified protein retained the full C-terminal Strep-tagII. Crystals were grown at 293 K by vapour diffusion in hanging drops, in which equal volumes of protein and well solutions were combined. The well solution was composed of 1.6 *M* ammonium sulfate and 150 m*M* sodium citrate pH 7.0. $CuSO_4$ was added to the protein solution in a twofold molar excess prior to mixing with the precipitant. Large crystals of crystal forms II and IV (Freeman *et al.*, 1996; Kishishita *et al.*, 2003; Langley *et al.*, 2006) grew routinely in two weeks.

2.2. X-ray data collection and refinement

Prior to cryocooling, crystals were derivatized and protected for freezing using the following protocol. Well solution was added to hanging drops containing crystals to bring the total drop volume to 20 µl. The drop with the crystals was then transferred to a sitting-drop well and the volume was increased to 30 µl by the further addition of well solution. Well solutions supplemented with added glycerol in 5%(*v*/*v*) increments were then exchanged for half the sitting-drop volume until the final glycerol concentration was approximately 30%(*v*/*v*). This involved 12 solution exchanges (two per glycerol increment) over a period of 2 h, after which crystals were cryocooled in a cold nitrogen stream. The BH complex was prepared by soaking a cryoprotected crystal in well solution containing 30%(*v*/*v*) glycerol and 2 m*M* BH (benzylhydrazine dihydrochloride; Sigma, without further purification) for a further 15 min before cryocooling. The conditions corresponded to an ∼200-fold molar excess of BH over AGAO active sites. Crystals of the TCP complex were prepared by first soaking crystals for 30 min in well solution containing 0.4 m*M* TCP [(±)-tranylcypromine hydrochloride; Sigma, without further purification]. (±)-Tranylcypromine, also termed (1*R*,2*S*)-*rel*-2-phenylcyclopropanamine, is a mixture of (1*R*,2*S*)-2-phenylcyclopropanamine and (1*S*,2*R*)-2-phenylcyclopropanamine. The cryoprotection procedure was then followed, using solutions to which the same concentration of TCP had been added.

X-ray data were recorded on a MAR Research 345 mm image-plate detector with X-rays generated from a Rigaku RU-200/HR rotating-anode generator with a copper target (λ = 1.54 Å) and Osmic mirror optics. All data were recorded from crystals maintained at 100 K in a stream of cold nitrogen gas (Oxford Cryosystems). Data were integrated and scaled with *DENZO* and *SCALEPACK*, respectively, from the *HKL* suite of programs (Otwinowski & Minor, 1997)

The structure of the TCP complex was solved by molecular replacement using *MOLREP* (Vagin & Teplyakov, 1997). The search model was a dimer created from the refined 1.55 Å native structure using crystallographic symmetry (Langley *et al.*, 2006) with all metal ions and solvent molecules removed and with the cofactor modelled as alanine. The same starting model was used to commence the refinement of the BH complex. Following initial rigid-body optimization, refinement protocols for both structures comprised cycles of refinement with *REFMAC*5 (Murshudov *et al.*, 1997), addition of water molecules with *ARP*/*wARP* (Perrakis *et al.*, 1999), checks of the model in electron density ($F_{obs} - F_{calc}$ and $2F_{obs} - F_{calc}$ maps) and the addition/deletion of water molecules and metal ions if they were located in significant electron density and made satisfactory hydrogen-bond or ligand interactions. Graphical manipulation of the models and inspection of electron-density maps were carried out with *O* (Jones *et al.*, 1991). The TPQ cofactors were modelled only in the final stages of the refinement. The TPQ adducts formed by BH and

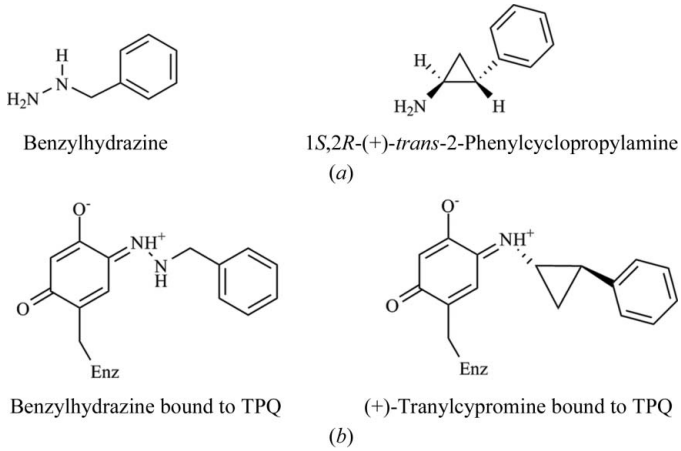

Figure 1
Chemical structures (*a*) of the inhibitors BH and (+)-TCP or (1*S*,2*R*)-2-phenylcyclopropanamine and (*b*) of their adducts with TPQ.

Table 1
X-ray data statistics for AGAO complexes of TCP and BH.

Values in parentheses are for the highest resolution shell.

	TCP complex	BH complex
Crystal form†	IV	II
Space group	*I*2	*C*2
Unit-cell parameters		
a (Å)	158.11	158.13
b (Å)	63.00	62.67
c (Å)	184.49	92.28
β (°)	112.0	112.1
No. of subunits per ASU	2	1
Resolution range (Å)	28.0–1.65	28.0–1.86
Completeness (%)	98.2 (80.0)	93.4 (75.2)
Redundancy	7.4	3.0
$\langle I/\sigma(I)\rangle$	15.7 (3.0)	12.6 (2.4)
$R_{\rm merge}$‡	0.062 (0.459)	0.065 (0.408)

† Three different forms of AGAO crystals were initially characterized (Freeman *et al.*, 1996); a fourth in space group *I*2 was described subsequently (Kishishita *et al.*, 2003). We have chosen the unconventional space-group setting *I*2 for ease of comparison with previously published structures by others. The relationship between the structures in the different crystal forms has been detailed previously (Langley *et al.*, 2006). ‡ $R_{\rm merge} = \sum_{hkl}\sum_i |I_i(hkl) - \langle I(hkl)\rangle|/\sum_{hkl}\sum_i I_i(hkl)$.

Table 2
X-ray refinement statistics.

Values in parentheses are for the highest resolution shell.

	TCP complex	BH complex
No. of reflections used in refinement	190612	62670
No. of reflections for $R_{\rm free}$	10049 (758†)	3312 (207‡)
Composition of the final model		
Protein residues	*A*9–*A*627, *B*9–*B*627	*A*9–*A*628
Protein atoms (non-H)	*A*, 4873; *B*, 4873	4881
Residues with alternate conformers	*A*, 2; *B*, 2	1
Solvent atoms	488	503
Metal ions	*A*, 1 Cu, 1 Na; *B*, 1 Cu, 1 Na	1 Cu, 1 Na
Sulfate ions	*A*, 1; *B*, 1	3
Glycerol molecules	*A*, 4; *B*, 5	5
Inhibitor molecules	*A*, 1; *B*, 1	1
$\langle B\rangle$, protein atoms (Å^2)	A: 19B: 12	16
$\langle B\rangle$, solvent atoms (Å^2)	41	41
$\langle B\rangle$, metal ions (Å^2)	28	31
$\langle B\rangle$, TPQ side chain (Å^2)	*A*, 22; *B*, 15	20
$\langle B\rangle$, inhibitor atoms (excluding TPQ atoms) (Å^2)	*A*, 27; *B*, 23	28
$R_{\rm cryst}$§	0.172 (0.262)	0.162 (0.283)
$R_{\rm free}$¶	0.199 (0.269)	0.191 (0.320)
Ramachandran plot analysis††		
Allowed (%)	99.6	99.5
Favoured (%)	96.8	96.8
Outliers (%)	0.4	0.5
ESU based on maximum likelihood‡‡ (Å)	0.06	0.08
DPI§§ (Å)	0.07	0.11
PDB code	1w4n	1w5z

† Reflections for the free *R* set were chosen randomly without accounting for possible bias arising from noncrystallographic symmetry relationships. ‡ The same reflections were chosen for the free *R* set as used in the previous refinement of the native structure in this cell (Langley *et al.*, 2006) to avoid bias. § $R_{\rm cryst} = \sum_h |F_{\rm obs} - F_{\rm calc}|/\sum_h F_{\rm obs}$. ¶ $R_{\rm free}$ is calculated omitting approximately 5% of the reflections from the refinement calculations. †† Ramachandran plots were produced and analysed with *MOLPROBITY* (Lovell *et al.*, 2003). ‡‡ Estimated standard uncertainty from the *REFMAC* refinement (Murshudov *et al.*, 1997). §§ Diffraction precision indicator (Cruickshank, 1999).

TCP were represented in the refinement as modified amino-acid residues. They were constructed using the *PRODRG* (http://davapc1.bioch.dundee.ac.uk/prodrg/; Schüttelkopf & van Aalten, 2004) and *HicUP* (http://xray.bmc.uu.se/cgi-bin/gerard/hicup_server.pl) web servers and the libraries for *REFMAC* and *O* were generated using the *CCP*4*i* monomer library sketcher (Collaborative Computational Project, Number 4, 1994). Structures were validated using *PROCHECK* (Laskowski *et al.*, 1993), *WHATCHECK* (Hooft *et al.*, 1996) and *MOLPROBITY* (Lovell *et al.*, 2003).

3. Results

Each of the structures has been refined to reasonably high resolution and with good statistics and stereochemistry (Tables 1 and 2). The overall structures are virtually identical to the native structure of AGAO (PDB codes 1w6c and 1w6g; Langley *et al.*, 2006) and to each other. When the two independent chains of the TCP complex are superposed on each other or on the BH complex, the r.m.s.d. for C$^\alpha$ atoms ranges from 0.18 to 0.24 Å. The equivalent values for superposition on the native structures range from 0.25 to 0.34 Å. The TCP moeities in the two subunits of the TCP complex structure are in identical environments. The molecular structure of the dimer, indicating the location of the active-site cofactors, Cu atoms and entrance to the substrate funnels, is shown in Fig. 2.

3.1. Inhibitor-binding sites

The most obvious differences compared with the native structures occur around the active site and in the substrate-access funnel. The electron density for both inhibitor complexes (Figs. 3 and 4) unequivocally indicates the presence of a molecular fragment linked covalently to the C5 position of the TPQ cofactor. In both structures the TPQ is in the 'off-Cu' conformation and is well ordered as indicated by the electron density and the relatively low *B* factors (Table 2). This finding contrasts with the situation in the native structures, in which the side chain of TPQ is frequently disordered

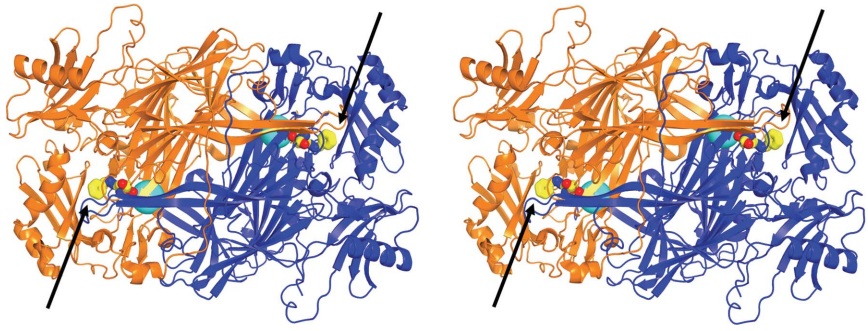

Figure 2
Stereoview of the AGAO dimer viewed along the twofold molecular axis. The subunits are coloured blue and gold. The Cu atom is shown as a cyan sphere. The BH adduct of the TQP cofactor is shown in ball-and-stick representation. The location of the active site in each subunit is indicated by an arrow.

(Langley *et al.*, 2006). In the 'off-Cu' conformation (originally called 'TPQ-off'; Wilce *et al.*, 1997) the TPQ is not coordinated to the Cu atom, in contrast to the 'on-Cu' conformation (see also Fig. 5).

The complexes of BH and TCP are modelled as substrate Schiff-base adducts with TPQ (Fig. 1). Formation of a Schiff base in the TCP complex is consistent with the observation of a chromophore with a λ_{max} at 350 nm (Shepard *et al.*, 2003). The TPQ cofactor has the same position and orientation in the two structures. The phenyl ring of both inhibitors lies in the same plane; the ring of TCP extends further towards the protein surface than that of BH as a consequence of the extra atom in the chain linking the ring to the TPQ (Fig. 5). For the TCP complex, which was prepared by soaking AGAO crystals in a racemic mixture of the TCP enantiomers, the electron density indicates that the (+)-enantiomer is preferentially bound. The same enantioselectivity was observed in the ECAO complex of TCP (Wilmot *et al.*, 2004).

It has been suggested that Tyr296 is a 'gate' that opens to allow substrate to access the TPQ cofactor (Wilce *et al.*, 1997). A comparison between the positions of Tyr296 in the native structure of AGAO and the BH and TCP complexes shows that the 'gate' is open when inhibitors are covalently attached to the TPQ (Figs. 5 and 6). Atoms of TCP and BH would clash with Tyr296 if it remained in its closed conformation. Another structural consequence of BH and TCP binding is a significant movement of Phe105, which lies inside the substrate-access funnel near the protein surface (Fig. 5). In the BH and TCP complexes the plane of the phenyl ring is rotated by $\sim$90° about χ_2 and the C^{α} atom has moved $\sim$1 Å compared with the native structure (Fig. 5). As a consequence, the phenyl group of

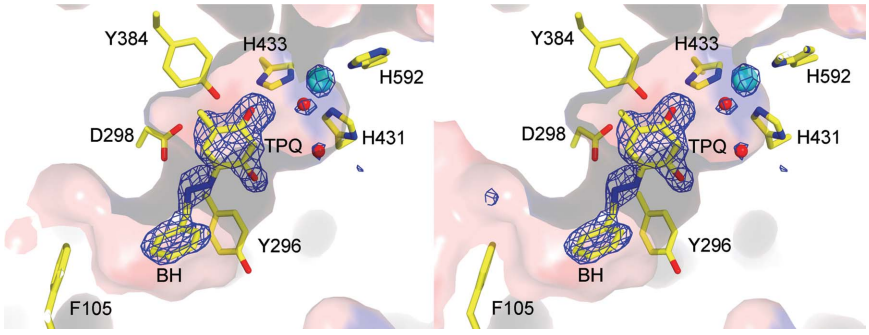

Figure 3
Stereoview of the active site of the BH complex of AGAO. The 'OMIT' electron density calculated without any contribution from the BH, TPQ, Cu atom or solvent molecules to the calculated structure factors is contoured at 4σ. The surface of the protein is coloured on the side facing the substrate-binding channel and grey looking from within the protein. The surface was calculated ignoring contributions from the TPQ and BH.

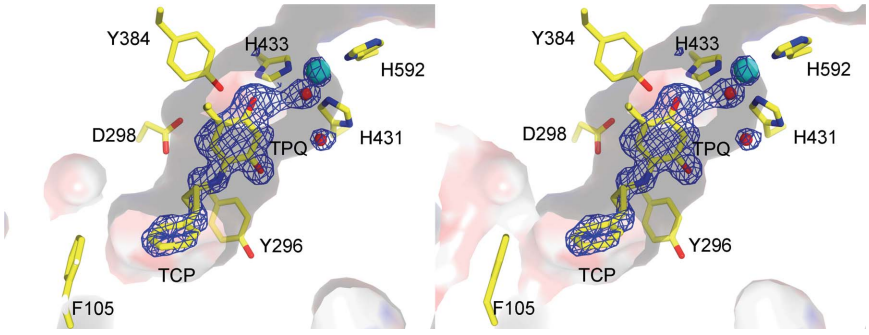

Figure 4
Stereoview of the active site of the TCP complex of AGAO. The 'OMIT' electron density calculated without any contribution from the TCP, TPQ, Cu atom or solvent molecules to the calculated structure factors is contoured at 4σ. The surface of the protein is coloured on the side facing the substrate-binding channel and grey looking from within the protein. The surface was calculated ignoring contributions from the TPQ and TCP.

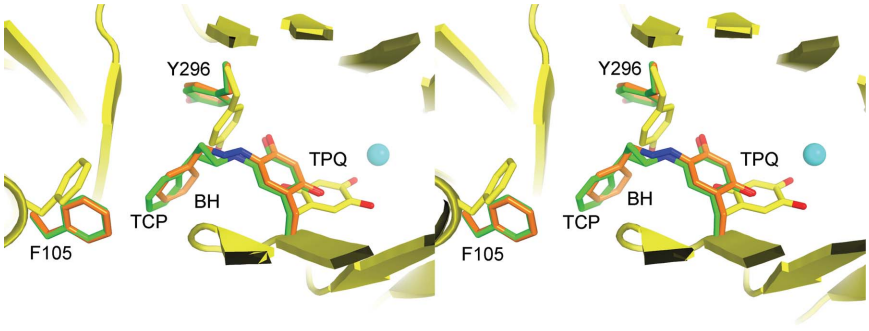

Figure 5
Stereoview showing selected residues in a superposition of the active sites of native AGAO (yellow C atoms) and its complexes with BH (orange C atoms) and TCP (green C atoms). The TPQ is in the 'on-Cu' conformation in the native structure and the 'off-Cu' conformation in the complexes. Movements of the gate Tyr296 to allow binding of the inhibitors and of Phe105 are evident.

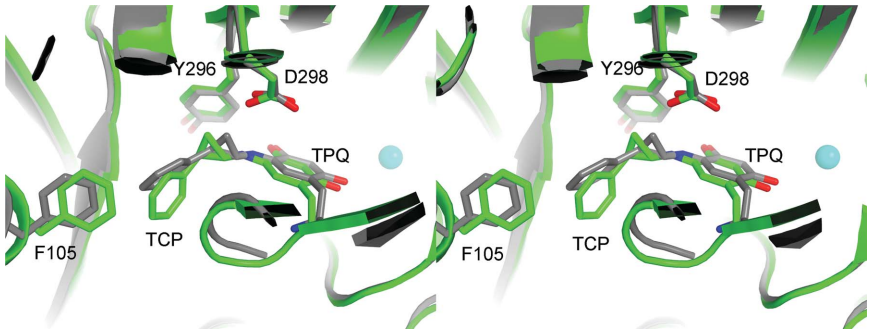

Figure 6
Stereoview showing selected residues in a superposition of the active sites of complexes of TCP with AGAO (green C atoms) and with ECAO (grey C atoms).

Phe105 moves nearly 3 Å to cap the active-site channel over the covalently bound inhibitors. The movement of the Phe105 side chain is accompanied by smaller movements in the polypeptide from Leu101 to Val108. The side chain of Glu106, which is disordered and cannot be modelled in the native structures, is clearly resolved in both the TCP and BH complexes. A hydrogen bond is formed between Glu106 $O^{\varepsilon 2}$ and Gln110 $N^{\varepsilon 2}$. There is no obvious reason why this hydrogen bond is not observed in the native structures, since both residues lie on the protein surface and are free to move.

The movement of the Tyr296 gate when BH or TCP is bound results in a movement of the side chain of Leu137, which lies on the opposite side of the channel to Phe105. Leu137 $C^{\delta 1}$ moves ∼1.5 Å from its position in the native structure in response to a close contact with Tyr296 O^{η} (3.3 Å in the TCP complex and 3.4 Å in the BH complex). As a consequence, there is also a small movement in the neighbouring residue Pro136.

3.2. Metal-binding sites

The three His ligands of the active-site Cu have a single conformation in the structures of both the BH and TCP complexes. An alternative conformation of His592 which occurs in the native structure of AGAO (Langley *et al.*, 2006) is not observed. Both the axial and equatorial water ligands of the active-site Cu are included in the model of the TCP complex, but only the axial water could be modelled in the BH complex. In other CuAO structures, the active-site Cu water ligands are frequently disordered or partially occupied (Duff *et al.*, 2006). Consequently, we do not draw any mechanistic inferences on the basis of these structures. An Na^{+} ion in the native structure (Langley *et al.*, 2006) is present in both the BH and TCP complexes. However, in contrast to the native structure, there is no evidence for exogenous Cu in the BH and TCP complex structures, despite the presence of excess $CuSO_4$ during crystal growth and cryoprotection.

4. Discussion

BH and TCP are effective inhibitors of AGAO. The structure analyses have shown that both inhibitors can form a covalent adduct linked to the C5 atom of the TPQ quinone ring. The inhibitors have apparently undergone the first part of the reductive half of the reaction cycle, forming a Schiff base (Shepard *et al.*, 2003). The structures and spectra of the adducts formed by TCP and 2-hydrazinopyridine (2-HP) with ECAO have been extensively characterized (Mure, Kurtis *et al.*, 2005; Mure, Brown *et al.*, 2005; Wilmot *et al.*, 2004; Saysell *et al.*, 2000). It is likely that the BH complex of AGAO is chemically equivalent to the hydrazone form of the 2-HP complex of ECAO (Mure, Brown *et al.*, 2005). This conclusion is supported by the formation of a hydrogen bond from Tyr284 O^{η} to TPQ O4 and by the fact that the methylene C atom of BH lies out of the plane of the TPQ ring.[1]

AGAO was originally named phenylethylamine oxidase, in recognition of its preference for substrates with an aromatic side-chain group. This preference is explained by a binding surface in the substrate channel that accommodates the aromatic rings of BH (this work), TCP (this work), 4-(aryloxy)-2-butynamines (O'Connell *et al.*, 2004) and the dimethylaniline group in Ru^{II} molecular wires (Contakes *et al.*, 2005). Interaction with the channel orients the aromatic ring of each inhibitor in the same plane.

Interestingly, ECAO was originally named tyramine oxidase after its preferred substrate, a breakdown product of tyrosine. Foods rich in tyramine (*e.g.* cheese), a substrate of human monoamine oxidase (MAO), the clinical target of MAO inhibitors, cause complications in patients treated with TCP. It has also been reported that tyramine inhibits the CuAO from lentil seedlings (LSAO; Padiglia *et al.*, 2004). In their proposed mechanism, tyramine is first oxidized by LSAO to an aldehyde, which spontaneously forms an adduct with the side-chain amino group of a lysine residue in the active-site cavity. They further suggested, based on the structure of AGAO, that tyramine may inhibit AGAO by derivatizing Lys184 and/or Lys354. AGAO is almost certainly capable of oxidizing tyramine since a TPQ–tyramine adduct has been trapped in an inactive mutant of AGAO in which the catalytic base Asp298 was substituted by alanine (Murakawa *et al.*, 2006). However, we see no evidence for inhibition by tyramine (data not shown) nor for any tyramine adduct when crystals of AGAO are soaked in an ∼500 molar excess of tyramine for one week (data not shown). It is possible to explain why tyramine inhibits LSAO and not AGAO based on the available structural data. LSAO shares 98% sequence similarity with pea-seedling amine oxidase (PSAO), the

[1] This conclusion is also supported by an additional structure of AGAO complexed with BH that has recently been deposited in the PDB without publication (PDB code 2e2v). This structure is of similar resolution (1.80 *versus* 1.86 Å). The crystals are of form IV like the TCP complex in the present work, with a dimer in the asymmetric unit compared with a monomer in our BH complex. The structure of the BH complex of AGAO reported here is essentially identical to that deposited as PDB entry 2e2v. The present structure of the BH–AGAO complex superposes on the *A* and *B* chains of 2e2v with a root-mean-square difference (r.m.s.d.) of 0.28 and 0.19 Å, respectively, for 602 well ordered C^{α}-atom positions. These values are similar to the value obtained when the *A* and *B* chains of 2e2v are superposed, namely 0.23 Å. The r.m.s.d. for the superposition of the 22 non-H atoms of the BH–TPQ adduct (residue 382) from our structure on the *A* and *B* chains of 2e2v are 0.25 and 0.17 Å, respectively. The Na^{+} ion included in our structure is modelled as water molecules in the two chains of 2e2v, despite overly short hydrogen-bond contacts and trigonal bipyramidal geometries.

structure of which is known. A lysine residue in PSAO is located in the same position in space but not in the secondary structure as the tyrosine residue in AGAO that forms a gate to the active site. Lys296 is conserved in PSAO and in LSAO and it is therefore likely that it is this lysine that is derivatized by the aldehyde product of tyramine oxidation. There are no lysine residues in AGAO closer than ∼10 Å to the active-site TPQ and even if these were modified it is unlikely that they would inhibit enzyme activity.

A comparison between the structures of the TCP complexes of AGAO and ECAO shows that the inhibitor is bound in the same manner (Fig. 6). However, there are small differences between the positions of the quinone ring of TPQ, the cyclopropane ring of TCP and the rotation of the phenyl ring of TCP (∼30° about the $C^{11}-C^{12}$ bond). In the ECAO–TCP complex the TCP is not fully occupied and atoms of the TCP phenyl ring have high *B* values (∼60 $Å^2$). This is consistent with the observation that TCP is a competitive inhibitor of ECAO with a measured K_i of ∼1 μ*M* (Saysell *et al.*, 2002). In contrast, in the AGAO–TCP complex the TCP is well ordered and the site is apparently fully occupied, in keeping with the observation that TCP is an incompletely reversible inhibitor of AGAO with an estimated IC_{50} of 38 μ*M* (Shepard *et al.*, 2003). Phenylhydrazine was able to displace TCP from AGAO (Shepard *et al.*, 2003). However, the reaction took much longer (15 *versus* 5 min) than in the absence of TCP. This is consistent with the structural observation that TCP effectively blocks the substrate channel of AGAO, limiting access by a competing inhibitor such as phenylhydrazine. In a study of the inhibition of six CuAOs [AGAO, bovine plasma AO (BPAO), equine plasma AO (EPAO), PPLO, human kidney diamine oxidase (HKAO) and pea seedling AO (PSAO)] the potency of TCP decreased in the order AGAO > BPAO > EPAO >> PPLO > PSAO > HKAO (Shepard *et al.*, 2003).

Only the (+)-TCP isomer is bound in the crystal structure of the AGAO complex. The orientation of the TCP cyclopropane ring is inappropriate for the abstraction of an H atom by the catalytic base (Asp298 in AGAO). Both of these observations were also reported for the TCP–ECAO complex (Wilmot *et al.*, 2004). Our results do not show whether the (−)-TCP isomer fails to bind or whether it is processed as a substrate and then removed from the active site.

The TPQ in all the structurally characterized inhibitor complexes of AGAO and ECAO is located in the 'off-Cu' position with similar orientations. This is true not only for the covalent adducts of TCP and BH described in this paper but also for members of the 4-(aryloxy)-2-butynamine family of mechanism-based inhibitors (O'Connell *et al.*, 2004) and for noncovalent molecular wires that act as competitive inhibitors of AGAO (Contakes *et al.*, 2005).

This work was supported by the Australian Research Council (DP0557353 to JMG, HCF and DMD) and by the National Institutes of Health, USA (GM27659 to DMD).

References

Airenne, T. T., Nymalm, Y., Kidron, H., Smith, D. J., Pihlavisto, M., Salmi, M., Jalkanen, S., Johnson, M. S. & Salminen, T. A. (2005). *Protein Sci.* **14**, 1964–1974.

Binda, C., Hubalek, F., Li, M., Herzig, Y., Sterling, J., Edmondson, D. E. & Mattevi, A. (2005). *J. Med. Chem.* **48**, 8148–8154.

Binda, C., Li, M., Hubalek, F., Restelli, N., Edmondson, D. E. & Mattevi, A. (2003). *Proc. Natl Acad. Sci. USA*, **100**, 9750–9755.

Cai, D. & Klinman, J. P. (1994). *J. Biol. Chem.* **269**, 32039–32042.

Collaborative Computational Project, Number 4 (1994). *Acta Cryst.* D**50**, 760–763.

Contakes, S. M., Juda, G. A., Langley, D. B., Halpern-Manners, N. W., Duff, A. P., Dunn, A. R., Gray, H. B., Dooley, D. M., Guss, J. M. & Freeman, H. C. (2005). *Proc. Natl Acad. Sci. USA*, **102**, 13451–13456.

Cruickshank, D. W. J. (1999). *Acta Cryst.* D**55**, 583–601.

Dove, J. E. & Klinman, J. P. (2001). *Adv. Protein Chem.* **58**, 141–174.

Dove, J. E., Smith, A. J., Kuchar, J., Brown, D. E., Dooley, D. M. & Klinman, J. P. (1996). *FEBS Lett.* **398**, 231–234.

Duff, A. P., Cohen, A. E., Ellis, P. J., Hilmer, K., Langley, D. B., Dooley, D. M., Freeman, H. C. & Guss, J. M. (2006). *Acta Cryst.* D**62**, 1073–1084.

Duff, A. P., Cohen, A. E., Ellis, P. J., Kuchar, J. A., Langley, D. B., Shepard, E. M., Dooley, D. M., Freeman, H. C. & Guss, J. M. (2003). *Biochemistry*, **42**, 15148–15157.

Duff, A. P., Trambaiolo, D. M., Cohen, A. E., Ellis, P. J., Juda, G. A., Shepard, E. M., Langley, D. B., Dooley, D. M., Freeman, H. C. & Guss, J. M. (2004). *J. Mol. Biol.* **344**, 599–607.

Freeman, H. C., Guss, J. M., Kumar, V., McIntyre, W. S. & Zubak, V. M. (1996). *Acta Cryst.* D**52**, 197–198.

Hooft, R. W. W., Vriend, G., Sander, C. & Abola, E. E. (1996). *Nature (London)*, **381**, 272.

Jakobsson, E., Nilsson, J., Ogg, D. & Kleywegt, G. J. (2005). *Acta Cryst.* D**61**, 1550–1562.

Jones, T. A., Zou, J.-Y., Cowan, S. W. & Kjeldgaard, M. (1991). *Acta Cryst.* A**47**, 110–119.

Juda, G. A., Bollinger, J. A. & Dooley, D. M. (2001). *Protein Expr. Purif.* **22**, 455–461.

Kim, M., Okajima, T., Kishishita, S., Yoshimura, M., Kawamori, A., Tanizawa, K. & Yamaguchi, H. (2002). *Nature Struct. Biol.* **9**, 591–596.

Kishishita, S., Okajima, T., Kim, M., Yamaguchi, H., Hirota, S., Suzuki, S., Kuroda, S., Tanizawa, K. & Mure, M. (2003). *J. Am. Chem. Soc.* **125**, 1041–1055.

Knowles, P., Kurtis, C., Murray, J. M., Saysell, C., Tambyrajah, W., Wilmot, C., McPherson, M., Phillips, S., Dooley, D., Rogers, M. & Mure, M. (2007). *J. Neural Trans.* **114**, 743–746.

Kumar, V., Dooley, D. M., Freeman, H. C., Guss, J. M., Harvey, I., McGuirl, M. A., Wilce, M. C. J. & Zubak, V. M. (1996). *Structure*, **4**, 943–955.

Langley, D. B., Duff, A. P., Freeman, H. C. & Guss, J. M. (2006). *Acta Cryst.* F**62**, 1052–1057.

Laskowski, R. A., MacArthur, M. W., Moss, D. S. & Thornton, J. M. (1993). *J. Appl. Cryst.* **26**, 283–291.

Li, R., Klinman, J. P. & Mathews, F. S. (1998). *Structure*, **6**, 293–307.

Lovell, S. C., Davis, I. W., Arendall, W. B. III, de Bakker, P. I., Word, J. M., Prisant, M. G., Richardson, J. S. & Richardson, D. C. (2003). *Proteins*, **50**, 437–450.

Lunelli, M., Di Paolo, M. L., Biadene, M., Calderone, V., Battistutta, R., Scarpa, M., Rigo, A. & Zanotti, G. (2005). *J. Mol. Biol.* **346**, 991–1004.

Matsunami, H., Okajima, T., Hirota, S., Yamaguchi, H., Hori, H., Kuroda, S. & Tanizawa, K. (2004). *Biochemistry*, **43**, 2178–2187.

Murakawa, T., Okajima, T., Kuroda, S., Nakamoto, T., Taki, M., Yamamoto, Y., Hayashi, H. & Tanizawa, K. (2006). *Biochem. Biophys. Res. Commun.* **342**, 414–423.

Mure, M., Brown, D. E., Saysell, C., Rogers, M. S., Wilmot, C. M., Kurtis, C. R., McPherson, M. J., Phillips, S. E. V., Knowles, P. F. & Dooley, D. M. (2005). *Biochemistry*, **44**, 1568–1582.

Mure, M., Kurtis, C. R., Brown, D. E., Rogers, M. S., Tambyrajah, W. S., Saysell, C., Wilmot, C. M., Phillips, S. E. V., Knowles, P. F., Dooley, D. M. & McPherson, M. J. (2005). *Biochemistry*, **44**, 1583–1594.

Murshudov, G. N., Vagin, A. A. & Dodson, E. J. (1997). *Acta Cryst.* D**53**, 240–255.

O'Connell, K. M., Langley, D. B., Shepard, E. M., Duff, A. P., Jeon, H.-B., Sun, G., Freeman, H. C., Guss, J. M., Sayre, L. M. & Dooley, D. M. (2004). *Biochemistry*, **43**, 10965–10978.

Okajima, T., Kishishita, S., Chiu, Y. C., Murakawa, T., Kim, M., Yamaguchi, H., Hirota, S., Kuroda, S. & Tanizawa, K. (2005). *Biochemistry*, **44**, 12041–12048.

Otwinowski, Z. & Minor, W. (1997). *Methods Enzymol.* **276**, 307–326.

Padiglia, A., Floris, G., Longu, S., Schinina, M. E., Pedersen, J. Z., Finazzi Agro, A., De Angelis, F. & Medda, R. (2004). *Biol. Chem.* **385**, 323–329.

Parsons, M. R., Convery, M. A., Wilmot, C. M., Yadav, K. D., Blakeley, V., Corner, A. S., Phillips, S. E., McPherson, M. J. & Knowles, P. F. (1995). *Structure*, **3**, 1171–1184.

Perrakis, A., Morris, R. & Lamzin, V. S. (1999). *Nature Struct. Biol.* **6**, 458–463.

Saysell, C. G., Murray, J. M., Wilmot, C. M., Brown, D. E., Dooley, D. M., Phillips, S. E. V., McPherson, M. J. & Knowles, P. F. (2000). *J. Mol. Catal. B Enzym.* **8**, 17–25.
Saysell, C. G., Tambyrajah, W. S., Murray, J. M., Wilmot, C. M., Phillips, S. E., McPherson, M. J. & Knowles, P. F. (2002). *Biochem. J.* **365**, 809–816.
Schüttelkopf, A. W. & van Aalten, D. M. F. (2004). *Acta Cryst.* D**60**, 1355–1363.
Shepard, E. M., Heggem, H., Juda, G. A. & Dooley, D. M. (2003). *Biochim. Biophys. Acta*, **1647**, 252–259.
Vagin, A. & Teplyakov, A. (1997). *J. Appl. Cryst.* **30**, 1022–1025.
Wilce, M. C. J., Dooley, D. M., Freeman, H. C., Guss, J. M., Matsunami, H., McIntire, W. S., Ruggiero, C. E., Tanizawa, K. & Yamaguchi, H. (1997). *Biochemistry*, **36**, 16116–16133.
Wilmot, C. M., Murray, J. M., Alton, G., Parsons, M. R., Convery, M. A., Blakeley, V., Corner, A. S., Palcic, M. M., Knowles, P. F., McPherson, M. J. & Phillips, S. E. (1997). *Biochemistry*, **36**, 1608–1620.
Wilmot, C. M., Saysell, C. G., Blessington, A., Conn, D. A., Kurtis, C. R., McPherson, M. J., Knowles, P. F. & Phillips, S. E. V. (2004). *FEBS Lett.* **576**, 301–305.